Wireless Netw (2014) 20:227–243
DOI 10.1007/s11276-013-0604-y

A placement mechanism for relay stations in 802.16j WiMAX networks

Chih-Yung Chang · Ming-Hsien Li

Published online: 30 May 2013

Abstract IEEE 802.16j standard defines Relay Station (RS) to enhance network throughput. Deploying RSs within the serving area of the Base Station (BS) could increase network throughput but raise the hardware cost problem. This paper presents a deployment algorithm for IEEE 802.16j network. According to the history traffic of internet usage, the proposed algorithm deploys as few as possible RSs at suitable locations such that the traffic requirement of each subarea can be satisfied. The proposed relay deployment algorithm mainly consists of three phases. The first phase aims to construct several promising zones where a RS deployed in each zone can improve the transmission rate from mobile station to BS. The second phase further combines several zones into a bigger one aiming at reducing the number of deployed RSs. The last phase selects the relay zones from the promising zones and deploys one RS in each relay zone. Simulation results show that our proposed algorithm can deploy the RSs at the most appropriate locations and hence efficiently reduce transmission delay and save the hardware cost.

Keywords WiMAX · IEEE 802.16j networks · Relay station

C.-Y. Chang (✉) · M.-H. Li
Department of Computer Science and Information Engineering, Tamkang University, Taipei, Taiwan
e-mail: cychang@mail.tku.edu.tw

M.-H. Li
e-mail: minghsienli@gmail.com

1 Introduction

WiMAX is an emerging advanced broadband wireless access technology which attracted a lot of attention in recent years. The IEEE 802.16e standard defines WiMAX network consisting of one Base Station (*BS*) and multiple Subscriber Stations (*SS*s) or Mobile Stations (*MS*s). The *BS* serves as a gateway between the WMAN and external networks and provides *MS*s and *SS*s with Internet access. In literature, there have been several studies [1, 2, 3] developing QoS scheduling frameworks for IEEE 802.16e networks. However, few existing works discussed the network deployment issue.

In considering the deployment issue in IEEE 802.16e networks, since all *SS*s and *MS*s directly connect to some *BS*s, a large number of *BS*s should be deployed to fully cover all service regions. To reduce the cost of deploying *BS*s, the relay station (*RS*) interconnected between the *BS* and *MS*s (or *SS*s) is proposed in the new version of IEEE 802.16j standard [4]. In the IEEE 802.16j networks, the *BS* is in charge of bandwidth assignment [5, 6] and routing [7] tasks for *RS*s, *MS*s or *SS*s. The standard of 802.16j defines two physical frames structures, including *transparent* and *non-transparent* modes. The transparent mode [8] aims to increase the system capacity while the non-transparent mode [9] is used to extend the coverage of the *BS*. In this work, we consider the transparent mode between the *BS* and *RS* and between *RS* and *SS*. The standard of IEEE 802.16j defines a frame in transparent mode consisting of downlink and uplink sub-frame. As shown in Fig. 1, the downlink sub-frame is further divided into access zone and transparent zone. In the time period of access zones, the *BS* could transmit data to *RS*s or *SS*s. Then *RS*s forward data to *SS*s during the time period of transparent zones. The *BS* might also directly

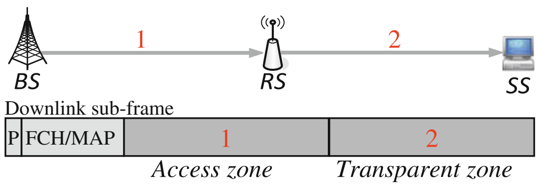

Fig. 1 Frame structure of IEEE 802.16j transparent mode and the transmission from *BS* to *SS* through *RS*

transmit its data to the *SS*s. Let *dst*(*A*, *B*) denote the distance between two stations *A* and *B*. Since the distances *dst*(*BS*, *RS*) and *dst*(*RS*, *SS*) are smaller than the distance *dst*(*BS*, *SS*), the data transmission rate from *BS* to *SS* can be enhanced. Therefore, how to determine the feasible locations for deploying *RS*s has received much attention recently.

IEEE 802.16 standard employs Modulation Coding Schemes (MCSs) for adjusting the transmission rate according to the channel condition. In a system with MCSs [10], stations closer to the *BS* are typically assigned higher order modulation with higher code rates. The modulation-order and/or code rate will be decreased as the distance from *BS* to the device increases. Table 1 summaries seven the MCSs and corresponding transmission rates. Let *L*(*A*, *B*) represent the link in the WiMAX network topology where stations *A* and *B* are sender node and receiver node, respectively. Let *dst*(*A*, *B*) denote the distance between two stations *A* and *B*. As shown in Fig. 2, assume that the value of *dst*(*BS*, *SS*) is 5,000(m), the feasible MCS and transmission rate applied to *BS* and *SS* would be QPSK 3/4 and 20.74Mbps, respectively. If the distance of *dst*(*BS*, *SS)* has been reduced to 2,000(m), the MCS could be changed to 16-QAM 3/4 to achieve better throughput. For those *SS*s that are far away from the *BS*, deploying a *RS* can reduce the distances between the *BS* and *RS* and between *RS* and *SS* and thus improve their transmission rates.

In literature, some researches [11, 12] proposed relay deployment mechanisms aiming at reducing the deployment cost and achieving full coverage. The work in [11] randomly generates several candidate locations for *BS*s and *RS*s. Then, the proposed mechanism decides the suitable locations from these candidate locations based on the traffic requirements of users. By considering the network throughput and signal strength policies, study [12] proposed two deployment schemes aiming at maximizing the network capacity. Although the existing work [11, 12] proposed relay placement algorithms for the purposes of minimizing network cost or maximizing capacity, the improper predefined location of *RS*s would reduce the performance of network planning.

Table 1 Modulation and coding schemes

Modulation and coding rate	Received SNR (dB)	Data rate (Mbps)	Distance range (m)
BPSK 1/2	6.4	6.91	$7{,}400 \le dst(a, b)$
QPSK 1/2	9.4	13.82	$5{,}220 \le dst(a, b) \le 7{,}399$
QPSK 3/4	11.2	20.74	$4{,}250 \le dst(a, b) \le 5{,}219$
16-QAM 1/2	16.4	27.65	$2{,}320 \le dst(a, b) \le 4{,}249$
16-QAM 3/4	18.2	41.47	$1{,}900 \le dst(a, b) \le 2{,}319$
64-QAM 2/3	22.7	55.30	$1{,}120 \le dst(a, b) \le 1{,}899$
64-QAM 3/4	24.4	62.21	$dst(a, b) \le 1{,}119$

This paper proposes an efficient relay placement mechanism aiming to minimize the number of required relay stations while the traffic requirements can be satisfied. The rest of this paper is organized as follows. Section 2 introduces the related works in developing relay deployment. The network model and problem formation are presented in Sect. 3. Section 4 proposes the relay placement mechanism while Sect. 5 investigates the performance improvements of the proposed mechanism against the existing works. Finally, Sect. 6 concludes this work.

2 Related work

Recently, a number of related works [11–15] proposed relay station placement schemes to cope with the *RS* deployment problems in a WiMAX network. To minimize the deployment cost, study [11] proposed another scheme which selects a number of the randomly determined candidate sites based on the integer programming technique. Then the proposed deployment scheme determines the feasible numbers of *BS*s and relay stations by considering the bandwidth requirements of *MS*s. However, the candidate sites are randomly determined. The network throughput will be degraded if the *RS*s are deployed at the randomly determined sites.

Some other *RS* deployment mechanisms were proposed by considering the feasible locations where the transmission rates can be improved. Wang et al. [12] aims at maximizing the network capacity by considering transmission rate and signal strength. To improve the network throughput, each *RS* will be deployed at a feasible location where the transmission rates of link *L*(*BS*, *RS*) and link *L*(*RS*, *MS*) are higher than that of *L*(*BS*, *MS*). However, the assumption that the *RS*s are regularly deployed around the *BS* may not achieve the optimal performance. In addition, the proposed algorithm does not consider that the available bandwidth of each *RS* will be decreased with the number of *MS*s connected to the same *RS*.

In addition to the improvement of network throughput, Lu et al. [13, 14] further considered the budget constraint and proposed a deployment strategy of *BS* and *RS*. This scheme assumes that the candidate *BS* and *RS* locations are known. It determines the best locations for *BS* and *RS* deployment while the hardware cost will not exceed the budget constraint. However, the pre-determined candidate locations may result in the degradation of network capacity.

Similar to previous studies [13, 14], Chang et al. [15] considered the budget constraint and proposed a relay deployment scheme aiming at maximizing the network throughput. Given k relays, the proposed deployment scheme partitions the network region into k subareas and then calculates the best location of *RS* in each subarea. This study takes into consideration frame structure of IEEE 802.16j and variable traffic demand required by each user. However, the proposed scheme might spend unnecessary cost on relay deployment since the predetermined number of *RS*s might larger than the number of required *RS*s in the networks.

This paper proposes an efficient relay placement mechanism aiming to minimize the number of required relay stations while the traffic demands can be satisfied. Compared with the existing deployment schemes, our proposed deployment mechanism can reduce the deployment cost by deploying fewer *RS*s at appreciate locations such that the contribution of each *RS* in rate enhancement can be maximized. Initially, a deployment scheme with minimal number of *RS* is proposed based on integer programming approach which takes into account the available bandwidth constraints of *BS* and *RS*s. Then a heuristic *RS* placement scheme is proposed to find feasible sub-regions for the deployment of *RS*s. Subsequently, the set of *RS*s is selected such that the number of *RS*s can be reduced and the traffic demands are satisfied. Simulation study reveals that the proposed scheme outperforms the existing approaches in terms of transmission delay, the number of deployed *RS*s and the computational cost.

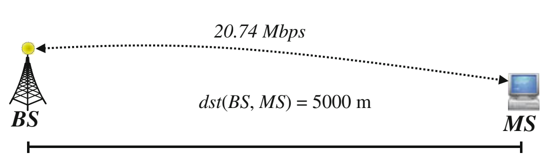

Fig. 2 The data rate between the *BS* and *MS* is highly depending on distance

3 Network environment and problem formulation

This paper considers a given WiMAX service area A where a single *BS* has been deployed at the center location of the area. As shown in Fig. 3, the network area A has been partitioned into a set of subareas $A = \{A_1, A_2, \ldots, A_n\}$. Assume that the traffic requirement d_i^{req} of each subarea A_i in each frame is known. The traffic requirements can be estimated according to the history traffic of the internet usage. The set of traffic requirements is denoted by $D = \{d_1^{req}, d_2^{req}, \ldots, d_n^{req}\}$. Let $BS(0, 0)$ denote the location of *BS*. Let CP_i denote the central request representing point of subarea A_i, and $A_i(x_i, y_i)$ denote the location of CP_i. Let $C = \{CP_1, CP_2, \ldots, CP_n\}$.

In a large network area, a single *BS* directly serving all users might lead to a situation that the traffic requirements of some users cannot be satisfied. The major reason is that the *MS* which has long distance to the *BS* can only adopt the lowest transmission rate and hence consumes a considerable bandwidth resource. To improve the network capacity, IEEE 802.16j incorporates functions of relay stations into WiMAX networks. Let $R = \{RS_1, RS_2, \ldots, RS_m\}$ denote the set of m candidate *RS*s, $m \le n$. This paper intends to develop a relay deployment mechanism which deploys as few as possible *RS*s for improving the average transmission rate of *MS*s but the traffic demands required by all subareas can be satisfied.

Herein, we notice that it is reasonable using the traffic demand of CP_i to represent the overall traffic requirement of subarea A_i. Assume that there are q users in the subarea A_i. Assume that each user has data requirement d_α and can apply transmission rate r_α, for $1 \le \alpha \le q$. For a given point CP_i, let p_i and d_i^{req} denote the applied transmission rate and the traffic requirement of CP_i, respectively. In fact, the CP_i can represent the overall traffic requirements in subarea A_i because that Expression (1) holds.

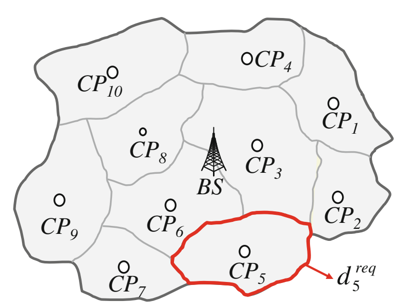

Fig. 3 The serving area of *BS* is partitioned into a set of subareas $A = \{A_1, A_2, \ldots, A_n\}$ and the central point of subarea A_i is denoted by CP_i

Table 2 Notation list

d_i^{req}	The traffic requirement of CP_i in a frame (*kb/frame*)
r_{BS-CP_i}	The transmission rate between BS and CP_i (*kb/slot*)
r_{BS-RS_j}	The transmission rate between BS and RS_j (*kb/slot*)
$r_{RS_j-CP_i}$	The transmission rate between RS_j and CP_i (*kb/slot*)
T^{DL}	The time interval of downlink subframe (*slots*)
$t_{A,B}^{req}$	The latency of required data transmission from stations A to B, where stations A and B might be either BS, RS or CP_i
t_i^{assign}	The time interval assigned to CP_i in a frame (*slots*)
l_i^{BS}	1: There existed a link between BS and CP_i 0: otherwise
$l_i^{RS_j}$	1: There existed a link between RS_j and CP_i 0: otherwise

$$d_i^{req} = \left(\sum_{\alpha=1}^{q} \frac{d_\alpha}{r_\alpha} \right) \times p_i \tag{1}$$

Table 2 lists a set of notations which will be used to present the network model and problem statements of this paper.

Let R_j^{deploy} be a Boolean value, which represents whether or not RS_j is deployed in subarea A_j. If yes, R_j^{deploy} is equal to 1. Otherwise, its value equals to zero. This paper aims at deploying as few as possible *RSs* at the best locations such that the network capacity can support all traffic requirements of *CPs*. Let N^{RS} denote the number of *RS*s deployed in the networks, where $N^{RS} \leq |R|$. Expression (2) gives the objective function while expressions (3)–(9) give constraints for the considered relay placement problem.

Objective function:

$$\text{Minimize}\, N^{RS} = \sum_{j=1}^{n} R_j^{deploy} \tag{2}$$

Subject to the following constraints:

$$\begin{aligned} r_{BS-CP_i} &= Tab^r(dst(BS, CP_i)) \\ r_{BS-RS_j} &= Tab^r(dst(BS, RS_j)) \\ r_{RS_j-CP_i} &= Tab^r(dst(RS_j, CP_i)), \quad \text{for}\, RS_j \in R \end{aligned} \tag{3}$$

where Tab^r is a function that queries Table 1 for the suitable MCSs and maps $dst(A, B)$ to the maximal transmission rate. Expression (3) depicts that the maximal transmission rates between CP_i and BS, RS_j and BS, and CP_i and RS_j can be derived by giving the distances of the communication pairs. In case that the condition $r_{BS-CP_i} > r_{RS_j-CP_i}$ is satisfied, deploying a relay cannot enhance the transmission rate of CP_i and thus the BS should directly communicate with *MS*s in subarea A_i. Alternatively, a relay RS_j might need to be deployed to serve as an intermediate forwarder node between the BS and CP_i.

The deployment of a relay between the BS and CP_i might reduce or increase the transmission latency of $L(BS, CP_i)$, depending on whether or not the deployed location of the relay is appropriate. Consider the following two scenarios. First, the traffic requirement d_i^{req} generated by CP_i is directly transmitted to BS. Second, there is a relay RS_j deployed between CP_i and BS. The data of requirement d_i^{req} generated by CP_i is firstly transmitted from CP_i to RS_j and then relayed from RS_j to the BS. In the first scenario, the latency between the BS and CP_i can be evaluated by

$$t_{BS,CP_i}^{req} = \frac{d_i^{req}}{r_{BS-CP_i}}. \tag{4}$$

In the second scenario, the latency between the BS and CP_i can be measured by the summation of the latency of the BS and RS_j and the latency of RS_j and CP_i. Therefore, the total latency from CP_i to the BS can be evaluated by

$$t_{BS,RS_j}^{req} + t_{RS_j,CP_i}^{req} = \frac{d_i^{req}}{r_{BS-RS_j}} + \frac{d_i^{req}}{r_{RS_j-CP_i}} \tag{5}$$

Consequently, the data transmission from CP_i to the BS through the relay forwarding can be more efficient only in case that the latency can be reduced. Constraint (6) reflects the constraint to this requirement.

$$t_{BS,RS_j}^{req} + t_{RS_j,CP_i}^{req} < t_{BS,CP_i}^{req} \tag{6}$$

Constraint (7) limits that a CP cannot connect to both the BS and RS at the same time.

$$l_i^{BS} + \sum_{j=1}^{m} l_i^{RS_j} = 1,\ \forall CP_i \in C \tag{7}$$

Constraint (8) gives a constraint that a deployed RS_j should connect to at least one CP.

$$R_j^{deploy} = \begin{cases} 1, & if\ \sum_{i=1}^{n} l_i^{RS_j} \geq 1, \quad \exists RS_j \in R \\ 0, & \text{otherwise} \end{cases} \tag{8}$$

Let T^{DL} denote the time interval of a downlink subframe. Constraint (9) depicts that the overall allocated transmission time of *CP*s cannot exceed the time interval of the downlink subframe.

$$T^{DL} \geq \sum_{i=1}^{n} t_i^{assign} \tag{9}$$

Constraint (10) constrains that the latency of data transmission from the BS to CP_i cannot exceed overall time interval assigned to CP.

$$\sum_{i=1}^{n} t_i^{assign} \geq \sum_{i=1}^{n} t_{BS,CP_i}^{req} + \sum_{i=1}^{n} \left(t_{BS,RS_j}^{req} + t_{RS_j,CP_i}^{req} \right), \forall RS_j \in R \quad (10)$$

Finally, Expression (11) depicts the flow constraint where the receiving traffic d_i^{req} of RS_j is equal to the transmitting traffic from itself to CP_i. This indicates that all input traffics of RS_j equal to all output traffics of RS_j.

$$\sum_{i=1}^{n} l_i^{RS_j} \times d_i^{req} = \sum_{i=1}^{n} \left[l_i^{RS_j} \times \left(t_i^{assign} - \frac{d_i^{req}}{r_{BS-RS_j}} \right) \times r_{RS_j-CP_i} \right], \quad \forall RS_j \in R \quad (11)$$

In the next Section, we will propose a cost-aware relay deployment mechanism which aims at achieving the goal presented in this Section and satisfying all constraints (2)–(11).

4 Cost-aware relay deployment (CARD) mechanism

This section introduces the proposed Cost-Aware Relay Deployment Mechanism (*CARD*). The mechanism aims at deploying as few as possible *RS*s at the appropriate locations while the network capacity can support all traffic requirements of each CP_i in each frame. The proposed *CARD* mainly consists of three phases. The first phase, called *Promising Zone Construction Phase,* aims at identifying the *Promising Zones,* which are candidate zones for deploying *RS*s. The second phase, called *Promising Zone Reduction Phase*, further combines the adjacent subareas into a larger one aiming at reducing the computing complexity for later phase. The third phase, called *Minimal Number of RSs Allocation Phase*, mainly allocates the minimal number of *RS*s to the feasible *Promising Zones* and guarantees that the traffic demands can be satisfied. The details designed in each phase are described as follows.

4.1 Promising zone construction (PZC) phase

Let *Promising Zone* Z_i denote the zone that deploying a *RS* within the zone can improve the transmission rate between CP_i and the *BS*. This phase aims at identifying the promising zone Z_i for each CP_i. In case that there does not exist the zone, it indicates that the CP_i should directly connect to the *BS*. Identifying the promising zones can significantly reduce the computing complexity of the relay deployment problem. Two steps will be executed in this phase. First, the *BS* explores the feasible MCSs for *RS*s and *CP*s that can improve the transmission rate between the CP_i and *BS*. The second step is to construct the promising zone according to adopted MCSs.

Recall that the deployment of a relay RS_j can enhance the transmission rate only if the latency from CP_i to *BS* through the relay forwarding can satisfy the constraint of (6). However, the transmission rates r_{BS-CP_i}, r_{BS-RS_j} and $r_{RS_j-CP_i}$ are mainly determined by the SINR values at the receiver sides, which are highly related to the distance between the sender and receiver. According to Table 1, the *BS* can adjust the MCS to maximize the transmission rate. Let m^{BS-CP_i}, m^{BS-RS_j} and $m^{RS_j-CP_i}$ denote the MCSs adopted by links $L(BS, CP_i)$, $L(BS, RS_j)$ and $L(RS_j, CP_i)$, respectively. The transmission rates r_{BS-CP_i}, r_{BS-RS_j} and $r_{RS_j-CP_i}$ can be derived by (3).

Figure 4 gives an example to illustrate this concept. The *BS* can derive the MCSs m^{BS-CP_i} and rate r_{BS-CP_i} by substituting the $dst(BS, CP_i)$ into function Tab^r. For any given placement location of RS_j along the straight line between the *BS* and CP_i, the MCS m^{BS-RS_j} and its corresponding transmission rate r_{BS-RS_j} can be estimated by substituting the distance $dst(BS, RS_j)$ to the function Tab^r. Similarly, the MCS $m^{RS_j-CP_i}$ and corresponding transmission rate $r_{RS_j-CP_i}$ can be obtained. Consequently, constraint (6) can be applied to check whether or not the given location is suitable for deploying a relay RS_j.

For a given location, (6) is able to determine whether or not it is located in the promising zone Z_i of the *BS* and CP_i. However, a big challenge to derive the promising zone is that the number of candidate locations is infinite. To derive the promising zones with a reasonable computing complexity, we consider the possible MCSs that can be applied to the RS_j. Let *M* be the number of predefined MCSs in IEEE 802.16j standard. To reduce the computational cost, the first step considers $M \times M$ cases.

In the first step of *Promising Zone Construction Phase*, the *CARD* tries to explore all possible MCSs which can be applied between the *BS* and RS_j and between RS_j and CP_i. Let *x* and *y* denote the sequence numbers of MCSs in Table 1. Let MCS pair $p_{xy}^i = \left(m_x^{BS-RS_j}, m_y^{RS_j-CP_i} \right)$ denote one of the $M \times M$ MCS pairs where $m_x^{BS-RS_j}$ and $m_y^{RS_j-CP_i}$ are the MCSs to be applied on the links (BS, RS_j) and (RS_j, CP_i),

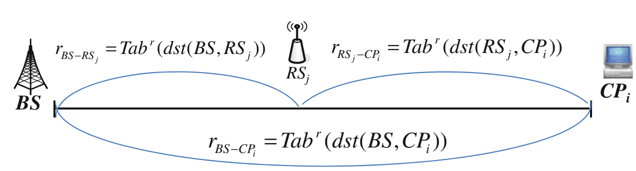

Fig. 4 The *CARD* can verify whether or not a given location is suitable for deploying RS_j

respectively. Let rate pair $r_{xy}^{i} = \left(r_{BS-RS_j}, r_{RS_j-CP_i}\right)$ denote the corresponding rates of MCS pair$\left(m_x^{BS-RS_j}, m_y^{RS_j-CP_i}\right)$. Substituting the rate pair into (6), the *CARD* can identify whether or not the MCS pair can be applied on the relay RS_j. Let Boolean variable f_{xy}^{i} be value 1 or 0, which represent whether or not r_{xy}^{i} satisfies (6), respectively. That is,

$$f_{xy}^{i} = \begin{cases} 1, & \text{if } r_{xy}^{i} \text{ satisfies constraint} \\ 0, & \text{otherwise.} \end{cases} \quad (12)$$

With this identification, the step can collect all *feasible MCS pairs* in a *feasible MCS set* Ψ_i which will be the important basis for constructing the *Promising Zone* for CP_i in the next step. That is

$$\Psi_i = \left\{ p_{xy}^{i} \middle| f_{xy}^{i} = 1, \forall m_x, m_y \in M \right\} \quad (13)$$

As a result, we can derive the feasible MCS set which will be further used in the next step.

In the second step of *Promising Zone Construction Phase*, the *proposed CARD mechanism* initially partitions the *BS*'s serving area *A* into *M* coronas as shown in Fig. 5. The width of each corona is determined based on the transmission distance of each MCS. Let $A_m^{BS-RS_j}$ denote the corona region where the MCS *m* is adopted on link (*BS*, RS_j). Similarly, the proposed *CARD* mechanism partitions the area of each CP_i's communication range into adjacent coronas according to the corresponding distance of each MCS. Let $A_m^{RS_j-CP_i}$ denote corona region where the MCS *m* is adopted on link (RS_j, CP_i). According to the feasible MCS pair $p_{xy}^{i} = \left(m_x^{BS-RS_j}, m_y^{RS_j-CP_i}\right)$, this step can construct an *intersection area* a_{m_x,m_y}^{i} of $A_{m_x}^{BS-RS_j}$ and $A_{m_y}^{RS_j-CP_i}$. The area marked with green color in Fig. 6 gives an example to illustrate the *intersection area* $A_{16QAM1/2}^{BS-RS_j} \cap A_{16QAM1/2}^{RS_j-CP_1}$ between the *BS* and CP_i, which is constructed based on the feasible MCS pair (16QAM 1/2, 16QAM 1/2).

Since each MCS pair can contribute an intersection area, the union of these areas will further form a larger promising zone Z_i *of* CP_i, which can be derived by expression (14).

$$Z_i = \bigcup_{m_x, m_y \in \Psi_i} a_{m_x,m_y}^{i} \quad (14)$$

In this step, the proposed *CARD* mechanism repeatedly executes the same procedure to construct the intersecting area a_{m_x,m_y}^{i} until promising zone Z_i of CP_i is constructed. Figure 7 gives an example to apply another feasible MCS pairs (16QAM 3/4, 16QAM 1/2) in step 2 of the *Promising Zone Construction Phase*. Hence, the *BS* and CP_i have the second *intersection area* $a_{16QAM3/4,16QAM1/2}^{i}$ as marked by blue color. Assume that the two coronas have a nonempty intersection area. Since the exchange of the two coronas also has the same size of intersection area, the MCS pair p_{xy}^{i} constructing an intersection area a_{m_x,m_y}^{i} also indicates that the pair p_{xy}^{i} can also construct an intersection area a_{m_y,m_x}^{i}. Therefore, the promising zone Z_1 of CP_1 contains three intersection areas which are marked with one green area and two blue areas as shown in Fig. 8.

Let P^Z denote the set of promising zones *of* all *CP*s. By applying the two steps of *Promising Zone Construction Phase*, the proposed *CARD* mechanism can identify promising zone P^Z for all CP_i. It also is worthy to notice that constraint (8) can be satisfied by deploying a *RS* within a promising zone. Figure 9 gives an example to illustrate the constructed promising zones. As shown in Fig. 9, the two steps of *Promising Zone Construction Phase* are executing on ten *CP*s. Some *CP*s cannot establish the promising zone. The major reason is that these *CP*s obtain less throughput if they transmit data to the *BS* through *RS*s.

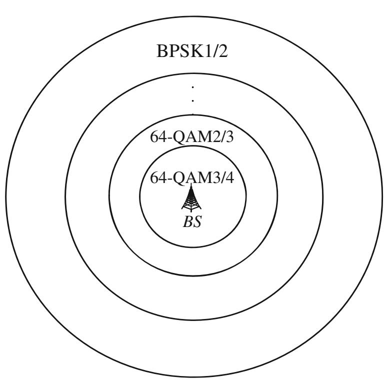

Fig. 5 The serving area of the *BS* partitions into *M* coronas

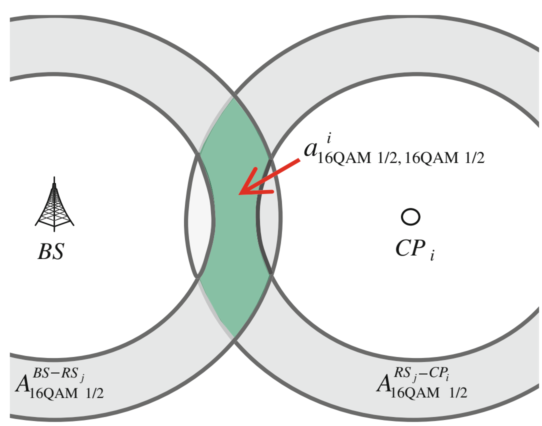

Fig. 6 The promising zone of CP_i

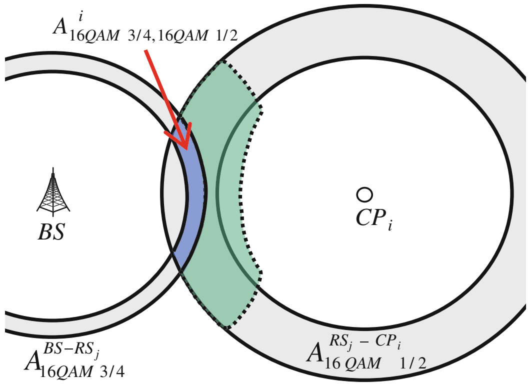

Fig. 7 The step 2 of *Promising Zone Construction Phase* constructs second intersection area

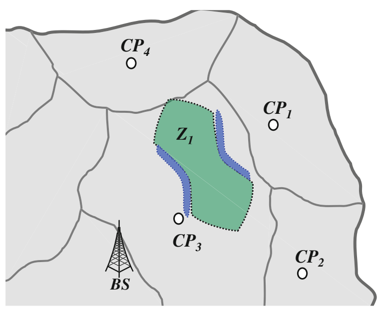

Fig. 8 An example of *Promising Zone Construction* for CP_1

Figure 10 details the procedure of the proposed *Promising Zone Construction Phase*. In steps 1–5, the *CARD* explores the feasible MCS set Ψ_i, referred to (13). In step 8, notation C^R represents the set of *CP*s which are suitable to connect to *RS*s. Steps 6–10 identify the set C^R. It is notable that *CP*s not belonging to C^R will directly connect to the *BS*. As a result, constraint (7) can be satisfied. Steps 11–18 of the main procedure construct the promising zone Z_i to each CP_i in C^R and then collect the constructed zones in the P^Z.

4.2 Promising zone reduction (PZR) phase

This section presents the *Promising Zone Reduction Phase* which aims at eliminating promising zones for further reducing the computational cost of later phase. The main idea is to deploy a *RS* within the overlapped area of multiple promising zones such that one *RS* can serve multiple *CP*s. As shown in Fig. 11, by applying the *Promising Zone Construction Phase* as described in previous section, the proposed *CARD* mechanism constructs promising zones Z_1 and Z_2 for CP_1 and CP_2, respectively. In case that one relay is deployed in each promising zone, two relays are required. The two zones intersect to form a small region which is marked by red shadow color. When a *RS* is deployed in the shadow region, it can commonly serve both

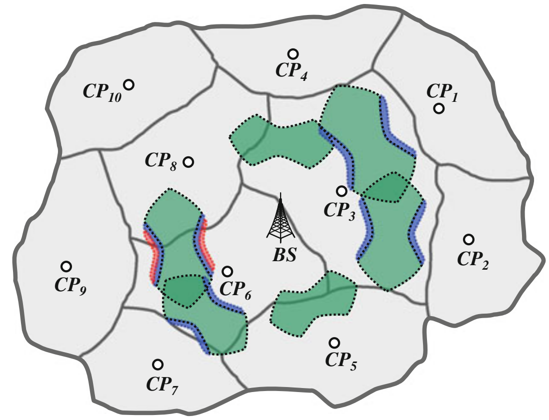

Fig. 9 An example of the promising zones which are successfully constructed for some *CP*s

CP_1 and CP_2. Instead of deploying one *RS* in each promising zone, deploying one *RS* in the shadow region can reduce the hardware cost of relay deployment.

Let O_Φ denote an *overlapped area* of a set of *k Promising Zone*s Z_1, …, Z_k, where $\Phi = \{1, \ldots, k\}$. Let $A_\Phi = \{A_1, \ldots, A_k\}$ denote the set of subareas whose corresponding promising zones Z_1, …, Z_k have a common overlapped area O_Φ. Let RS_Z denote the *RS*s that will be deployed in the overlapped region O_Φ. As shown in Fig. 11, let $RS_{\{1,2\}}$ to be the *RS* deployed in the overlapped region $O_{\{1,2\}}$. Since $RS_{\{1,2\}}$ falls in Z_1 zone, it can satisfy the rate constraint as depicted in (6). That is, the time required for data transmissions from CP_1 to the *BS* through $RS_{\{1,2\}}$ is smaller than that required for data transmission directly from CP_1 to the *BS*. Similarly, the $RS_{\{1,2\}}$ also falls in Z_2 zone, which indicates that the $RS_{\{1,2\}}$ is suitable to be a forwarder between CP_2 and the *BS*. As a result, the relay $RS_{\{1,2\}}$ can serve all *MS*s fallen in both regions A_1 and A_2. Therefore, merging subareas A_1 and A_2 into a bigger area $A^{merge}_{\{1,2\}}$ can save one relay, as compared with the deployment policy that deploys one relay at each promising zone of Z_1 and Z_2. Let A^{merge}_{Φ} denote the bigger area which merges all subareas in the set A_Φ. To reduce the number of required relays, in this phase, a merging process will be developed for combining the set of k subareas $A_\Phi = \{A_1, \ldots, A_k\}$ into a bigger region $A^{merge}_{\{1,\ldots,k\}}$. Then the *Promising Zone Construction Phase* should be again applied to derive the new promising zone of the merged subarea $A^{merge}_{\{1,\ldots,k\}}$.

From the observation of Fig. 11, merging overlapped subareas A_i and A_j into a bigger subarea $A^{merge}_{\{i,j\}}$ can help reduce the number of required *RS*s. However, the overlapped relation between subareas might be complicated. A general merging process should be developed to cope with all complicated cases. Let g_Φ denote the *overlapped degree* of O_Φ, and its value is the number of promising zones in the

Fig. 10 Algorithm of *Promising Zone Construction Phase*

Zone_Contruction(*C*, *D*, *BS*)

Input : A set of CP_i, traffic requirement d_i^{req} of each subarea A_i and the location of *BS*.

Output : C^R and a promising zones set P^Z.

For each $CP_i \in C$ **do**
  For each $(m_x^{BS-RS_j}, m_y^{RS_j-CP_i})$ where $m_x, m_y \in M$
    If $(m_x^{BS-RS_j}, m_y^{RS_j-CP_i})$ satisfies (6) **do**
      Add $(m_x^{BS-RS_j}, m_y^{RS_j-CP_i})$ to Ψ_i //referred to (13)
    End If
  End
  If Ψ != *null* **do**
    $C^R = C^R \cup CP_i$;
  End If
End
For each $CP_i \in C^R$ **do**
  For $l = 1$ to $|\Psi_i|$
    Partition $A_{m_x}^{BS-RS_j}$ and $A_{m_y}^{RS_j-CP_i}$ based on $(m_x^{BS-RS_j}, m_y^{RS_j-CP_i})$;
    $a^i_{m_x, m_y} = A_{m_x}^{BS-RS_j} \cap A_{m_y}^{RS_j-CP_i}$; //referred to (14)
    $Z_i = Z_i \cup a^i_{m_x, m_y}$;
    $P^Z = P^Z \cup Z_i$;
  End
End
return (C^R, P^Z);

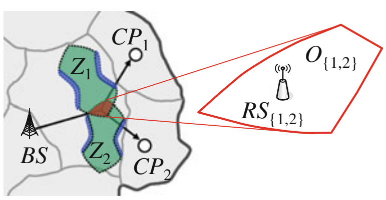

Fig. 11 The *RS* deployed in the overlapped region $O_{\{1,2\}}$ of Z_1 and Z_2 can reduce the hardware cost of relay deployment

set Φ. This phase initially finds A_Φ whose overlapped region O_Φ has highest overlapped degree g_Φ. Then the merging process, called *Merge*(A_Φ), will be applied to merge all subareas A_i, …, A_k in the subarea set A_Φ, in order to form a bigger subarea $A_q^{merge} = A_\Phi^{merge}$, where q is a new assigned number, starting from 1, of the merged subarea. After, the *CARD* will calculate the new central request representing point, called CP_q^{merge}, in the merged area A_q^{merge} and then apply Phase I to derive the new promising zone Z_q^{merge} of subarea A_q^{merge}. The merging process will be repeatedly executed until none of promising zone has overlapped area.

Figure 12 gives an example of the execution of *Promising Zone Reduction Phase*. In Fig. 12(a), the processes in the previous *Promising Zone Construction Phase* construct promising zones Z_1, Z_2 and Z_3 for CP_1, CP_2 and CP_3, respectively. As shown in Fig. 12(b), because the overlapped region $O_{\{1,2,3\}}$ has the highest overlapped degree $g_{\{1,2,3\}}$, this phase prior merges the subarea A_1, A_2 and A_3 into a merged subarea $A_1^{merge} = A_{\{1,2,3\}}^{merge}$. Afterward, the *BS* recalculates the new CP_1^{merge} and the new promising zone Z_1^{merge} for CP_1^{merge}. Finally, this phase terminates because none of promising zone overlaps with other zones.

Figure 13 describes the details of the proposed *Promising Zone Reduction Phase*. Let Z^M denote the set of new merged promising zones by applying the *Promising Zone Reduction Phase*. Let CP^M denote the set of *CP*s corresponding to the promising zones in Z^M. In step 1, the initial values of Z^M and CP^M are set to be empty. In steps 2 $\sim$ 7, the *BS* combines subareas until none of *Promising Zone* has overlapped region. The step 8 recalculates *CP* of the combined subarea. Finally, step 13 returns the sets Z^M and CP^M.

4.3 Minimal number of RSs allocation (MRA) phase

In the previous subsections, the steps of proposed *Promising Zone Construction Phase* have constructed the promising zone for each *CP* while the operations of *Promising Zone Reduction Phase* further reduce the number of promising zones by merging those neighboring subregions whose promising zones have common overlapped region. The *MRA* phase proposed in this section aims to further reduce the number of *RS*s. Let Z^M denote the set of new promising zones by applying the previous

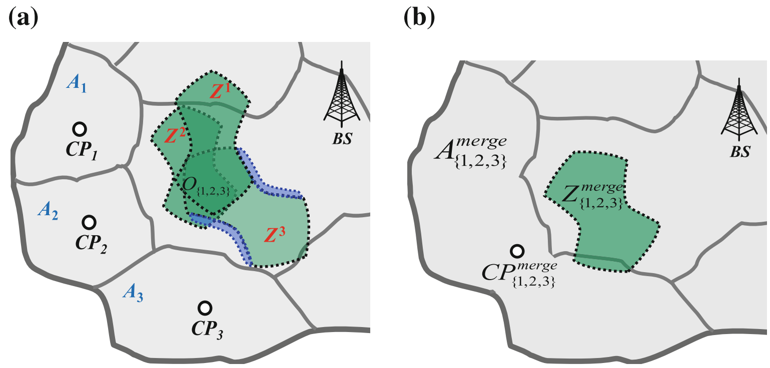

Fig. 12 **a** An example of network without applying *Promising Zone Reduction Phase*. **b** The number of promising zones is reduced after applying *Promising Zone Reduction Phase*

Fig. 13 Algorithm of *Promising Zone Reduction Phase*

Zone_Reduction(C^R, P^Z)

Input : A set C^R and a promising zone set P^Z

Output : CP^M and Z^M

CP^M=Φ; Z^M=Φ;
While there exists overlapped region O_Φ **do**
  Find A_Φ whose overlapped region O_Φ has highest overlapped degree g_Φ
  $A_\Phi^{merge} = Merge(A_\Phi)$;
  $A = A - A_\Phi$;
  $A = A \cup A_q^{merge}$;
  Compute new CP_q^{merge} of A_q^{merge};
  Run *Promising Zone Construction Phase*;
  Remove the *CP*s of A_Φ from C;
  $CP^M = CP^M \cup CP_q^{merge}$;
  $C = C \cup CP_q^{merge}$;
End
return (CP^M, Z^M);

two phases. Let CP^M denote the set of *CP*s corressponding to the promising zones in Z^M. The promising zones in Z^M are best candidates for deploying the *RS*s, however, it is not necessary to deploy a *RS* in each promising zones. Let ζ_{frame} denote the amount of data that the *BS* can support in a frame. Let $\zeta_{requirement}$ denote the total amount of data required by the serving area of the *BS*. In case that deploying *k* relays can reach the goal of $\zeta_{frame} \geq \zeta_{requirement}$, it is no need to further deploy any relay in any promising zone. Therefore, the goal of *Minimal Number of RSs Allocation Phase* is to cope with the problem that which promising zones need to deploy the *RS*s.

The following gives an example to illustrate the concept that how the proposed algorithm determines the deployment of relays such that the traffic requirements can be satisfied. As shown in Fig. 14, by applying the *Promising Zone Reduction Phase* as described in previous section, the *BS* combines the promising zones to form three new promising zone Z_1^{merge}, Z_2^{merge} and Z_3^{merge} for CP_1^{merge}, CP_2^{merge} and CP_3^{merge}. Figure 15 further gives three different deployments to illustrate the concept of the proposed algorithm. Assume each downlink interval T^{DL} contains 256 slots. Consider the deployment case (I) that none of *RS* is deployed in the network. That is, the *BS* can only directly communicate with each *CP*. Let the required transmission latencies t^{req}_{BS,CP_1}, t^{req}_{BS,CP_2} and t^{req}_{BS,CP_3} of links $L(BS, CP_1)$, $L(BS, CP_2)$ and $L(BS, CP_3)$ are 100, 70 and 125 slots, respectively. As shown in Fig. 15, without deploying any *RS*, the total required transmission timeslots are 295 slots/frame which is larger than 256 slots. Therefore, the bandwidth supported from *BS* cannot satisfy the downlink requirement. The deployment case (II) depicts another *RS* deployment where each promising zone is deployed one *RS*. With the *RS* deployment, we assume that the latencies required for transmitting data from *BS* to CP_1^{merge}, CP_2^{merge} and CP_3^{merge} through *RS* are 70, 45 and 110 slots, respectively. Thus the total transmission time of three *CP*s needs 225 (70 + 45 + 110) slots. As a result, the *BS* still have 31(256-225) available slots which is a wastage in bandwidth utilization. Compared with the deployment cases (I) and (II), deployment case (III) is the best deployment. In deployment case (III),

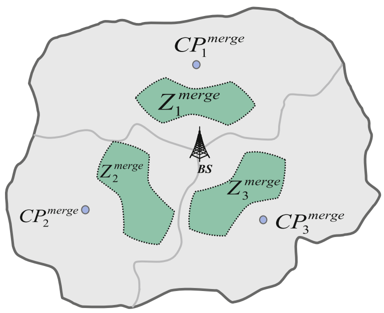

Fig. 14 An example of 802.16j networks by applying *Promising Zones Reduction Phase*

the *RS*s are deployed in *Promising Zones* Z_1^{merge} and Z_2^{merge}, and thus only the data transmission rates of CP_1^{merge} and CP_2^{merge} are improved. Therefore, the total time required for transmitting from three *CP*s to *BS* needs 240(70 + 45 + 125) slots/frame. As a result, the *BS* only remains 16(256-240) available slots. As compared to cases (I) and (II), the hardware cost of *RS*s is reduced while the *BS* satisfies the traffic demands.

Given a set of new promising zones Z^M by applying the operations designed in previous two phases, the *Minimal Number of RSs Allocation Phase* aims to identify a subset Z^{sub} of Z^M such that deploying a *RS* at each promising zone $Z_i^{sub} \in Z^{sub}$ can reduce the total number of *RS*s while the bandwidth of the *BS* satisfies the traffic requirements of serving area *A*. Let CP^{sub} denote the subset of *CP*s coeresponding to Z^{sub}. In order to minimize the number of *RS*s, the proposed algorithm aims at deploying *RS*s in the promising zone set Z^{sub} which has potential for increasing the network throughput. Let T^{over} denote the difference between the number of slots in each downlink subframe and the number of slots required for the *BS* directly transmitting its data to each *CP*. Expression (15) evaluates the value of T^{over}.

$$T^{over} = \sum_{i=1}^{n} t_{BS,CP_i}^{req} - T^{DL}, \forall CP_i \in C \tag{15}$$

Let t_i^b denote the *relay benefit* which represents the reduced transmission time if a *RS* is deployed in the merged zone Z_i^{merge} for CP_i^{merge}. The value of t_i^b can be further evaluated by applying Expression (16).

$$t_i^b = t_{BS,CP_i}^{req} - (t_{BS,RS_j}^{req} + t_{RS_j,CP_i}^{req}), \forall CP_i^{merge} \in CP^M \tag{16}$$

According to (16), the *MRA* phase calculates the *relay benefit* for each CP_i^{merge}. The larger value of t_i^b means that CP_i^{merge} can obtain more benefits from the relay deployment. Let $\Gamma = \left\{\hat{t}_1^b, \hat{t}_2^b, \ldots, \hat{t}_k^b\right\} = \left\{t_i^b, t_j^b, \ldots, t_k^b\right\}$ denote the set of the relay benefits of *CP*s belonging to CP^M in a decreasing order. Let $\Omega = \left\{\hat{Z}_1^{merge}, \hat{Z}_2^{merge}, \ldots, \hat{Z}_k^{merge},\right\} = \left\{Z_i^{merge}, Z_j^{merge}, \ldots, Z_k^{merge}\right\}$ denote the set of promising zones corresponding to Γ.

Based on the sequence of the set Γ, the proposed algorithm calculates the value of accumulated relay benefits of the first q promising zones $\hat{Z}_1^{merge}, \hat{Z}_2^{merge}, \ldots, \hat{Z}_q$, $q \le k$, where q should satisfy Expression (17) to guarantee that the transmission requirements of all *MS*s can be satisfied within each frame while the number of *RS*s is reduced. The satisfactory of (17) also indicates that constraints (9)–(11) can be satisfied.

$$\sum_{i=1}^{q} \hat{t}_i^b \ge T^{over}, \forall CP_i^{merge} \in CP^{sub} \tag{17}$$

Finally the operations of *MRA* phase deploy each *RS* at the appreciate location of each promising zone.

The following gives an example to illustrate the operations designed in *MRA Phase*. As shown in Fig. 16, in the previous phase, the number of promising zones in the serving region of *BS* has been reduced to six.

Fig. 15 The required transmission time of three case of *RS* deployment

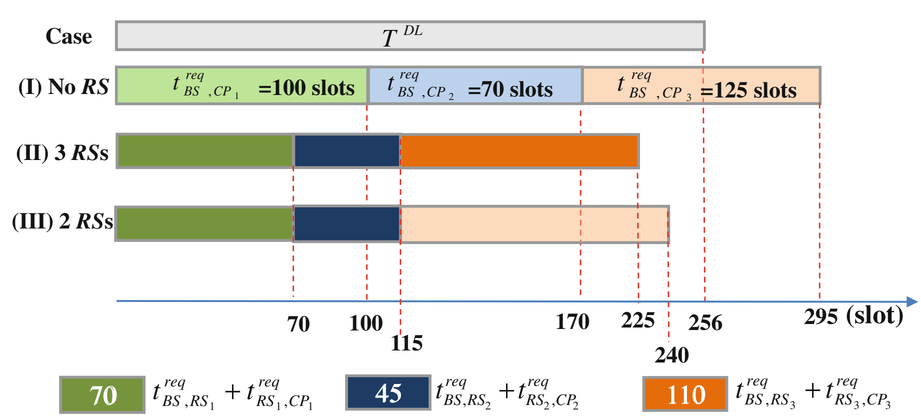

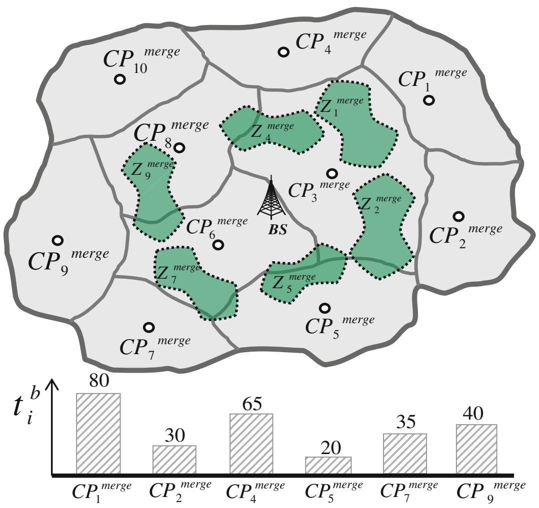

Fig. 16 An example of six *Promising Zones and their corresponding* relay benefit

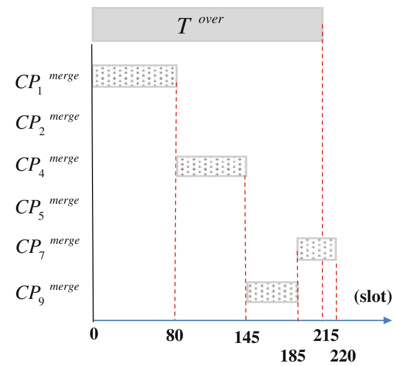

Fig. 17 The proposed *CARD* deploys four *RS*s by applying *Minimal Number of RSs Allocation Phase*

Without applying the operations designed in the *MRA* phase, there should be six *RS*s deployed in the severing region of *BS*. Assume that the relay benefits of CP_1^{merge}, CP_2^{merge}, CP_4^{merge}, CP_5^{merge}, CP_7^{merge} and CP_9^{merge} are 80, 30, 65, 20, 35 and 40 slots, respectively. Assume the value of T^{over} is 215 slots. As shown in Fig. 17, the proposed algorithm initially sorts all relay benefits and obtains $\Gamma = \left\{t_1^b = \widehat{t}_1^b, t_4^b = \widehat{t}_2^b, t_9^b = \widehat{t}_3^b, t_7^b = \widehat{t}_4^b, t_2^b = \widehat{t}_5^b, t_5^b = \widehat{t}_6^b\right\}$ and $\Omega = \left\{Z_1^{merge} = \widehat{Z}_1^{merge}, Z_4^{merge} = \widehat{Z}_2^{merge}, Z_9^{merge} = \widehat{Z}_3^{merge},\right.$ $\left.Z_7^{merge} = \widehat{Z}_4^{merge}, Z_2^{merge} = \widehat{Z}_5^{merge}, Z_5^{merge} = \widehat{Z}_6^{merge}\right\}$. After that, zones in Ω will be considered one by one in order, and be deployed a *RS* in the considered zone until Expression (17) is satisfied. Let the zone that has been determined to deploy a *RS* be called *relay zone*. For instance, the zone Z_1^{merge} is determined to be a relay zone and the accumulated relay benefit is 80 slots. Because the accumulated benefit is less than T^{over} (215 slots), the proposed algorithm continues to select Z_4^{merge} to play the role of relay zone. As a result, the relay benefit grows 65 slots. The accumulated relay benefit now achieves 145 slots. The similar operations will be applied and hence the zone Z_9^{merge} is selected to be relay zones. Since the selection of zone Z_7^{merge} results in a situation that the accumulated relay benefit is 220 slots and exceeds the T^{over}, the zone selection operations will be terminated. Consequently, zones $Z_1^{merge}, Z_4^{merge}, Z_9^{merge}$ and Z_7^{merge} are determined to be relay zones in the *MRA* phase. With the execution of operations designed in *MRA* phase, the total requirement of *CP*s can be satisfied while the number of *RS*s can be further reduced.

Figure 18 describes the procedure of *Minimal Number of RSs Allocation Phase*. Steps 1–4 calculate the total time required by all stations. Step 5 calculates the excess transmission time T^{over}. Steps 6–8 estimate the relay benefit t_i^b of each CP_i. Step 9 derives Γ by sorting the all relay benefits in a decreasing order. Steps 10–15 further allocate one *RS* at each Z_i^{merge} in a one-by-one manner for obtaining the maximal relay benefit until the accumulated relay benefit is larger than T^{over}. Finally, Step 16 returns the set of relay zones Z^{sub} and the number of deploying relays N^{RS}.

4.4 The algorithm of CARD

This section presents the proposed *Cost-Aware Relay Deployment mechanism* (*CARD*) algorithm. There are three phases designed in the main algorithm. As shown in Fig. 19, steps 1–5 setup the network environment which consists of one *BS*, a set of subareas, a set of *CP*s and traffic requirement of each *CP*. In Step 7, the function *Tab*^{r}, as referred to Table 1, applies the proper MCSs, and then maps *dst*(*BS*, CP_i) to the maximal transmission rate of link *L*(*BS*, CP_i). Step 8 measures the required transmission time of each CP_i, $1 \le i \le n$. Steps 11–13 further call three functions, namely *Zone_Contruction*(), *Zone_Merge*(), *Minimal_Number_RSs_ Allocation*(), as presented in the previous subsection, to determine the number of required *RS*s and the promising zones.

5 Simulation

This section presents the performance evaluation of the proposed relay deployment mechanism. The proposed *CARD* mechanism is compared with *Random* scheme which randomly deploys *RSs* in the *Promising Zones.* The proposed *CARD* mechanism also compares with the existing approaches proposed by studies [14] and [15]

Fig. 18 Algorithm of *Minimal Number of RSs Allocation Phase*

Minimal_Number_RSs_Allocation **(**C, CP^M, Z^M, D**)**

Input : C, A set of merged *CPs*, called CP^M , Z^M and D
Output : Z^{sub}, N^{RS}

$t^{temp} = 0$; benifit=0; j=1; CP^{sub}=Φ; N^{RS}=0; q=1;
For each $CP_i \in C$ **do**
  $t^{temp} = t^{temp} + t^{req}_{BS,CP_i}$;
End
$T^{over} = t^{temp} - T^{DL}$
For each $CP_i^{merge} \in CP^M$ **do**
  $t_i^b = t^{req}_{BS,CP_i} - (t^{req}_{BS,RS_j} + t^{req}_{RS_j,CP_i})$;
End
Sort all relay benefits and record the sequence in Γ and Ω;
While T^{over} > benefit **do**
  benefit=benefit+$\hat{t}_q^b$;
  CP^{sub} =$CP^{sub} \cup CP_i^{merge}$;
  Z^{sub} =$Z^{sub} \cup Z_i^{merge}$;
  $R_j^{deploy} = 1$; N^{RS}++; j++; q++;
End
return (Z^{sub}, N^{RS});

Fig. 19 *Cost-Aware Relay Deployment mechanism* (*CARD*)

Algorithm : Cost-Aware Relay Deployment Mechanism (*CARD*)

Create a location of BS.
Create a set of subareas $A = \{A_1, A_2, \ldots, A_n\}$.
Create a set of data request $D = \{d_1^{req}, d_2^{req}, \ldots, d_n^{req}\}$.
Find a set of CP_i *for subregion* A_i $C = \{CP_1, CP_2, \ldots, CP_n\}$.
Create a set of RS $R = \{RS_1, RS_2, \ldots RS_n\}$.
For each $CP_i \in C$ **do**
  $r_{BS-CP_i} = Tab^r(dst(BS, CP_i))$
  $t_i^{req} = d_i^{req} / r_{BS-CP_i}$;
End
Create a set C^R and P^Z .
(C^R, P^Z)=***Zone_Contruction***(C, D, BS);
(CP^M, Z^M)=***Zone_ Reduction*** (C^R, P^Z);
(Z^{sub}, N^{RS})=***Minimal_Number_RSs_Allocation***(C, CP^M, Z^M, D);
For *each* $Z_i^{merge} \in Z^{sub}$ do
  For k = 1 to N^{RS} do
    deploy RS_k in the Z_i^{merge};
  End
End

which are referred to as *TM-RSP* and *RPM*, respectively. In addition, an optimal scheme (*OPT*) which considers all possible cases of relay deployments is applied to investigate the performance of the proposed *CARD*. The simulator ns2 is used to evaluate the three compared deployment mechanisms. Table 3 gives the parameters considered in the simulation. The MCSs listed in Table 1 are applied in the simulations.

Figure 20 is a screenshot of the considered environment where the region size is set to 10 km × 10 km. One *BS* is deployed at the center of the service region. There are 300 users (*MS*s or *SS*s) randomly deployed in the

Table 3 Simulation parameters

Parameter	Value
Carrier frequency	5 GHz
System bandwidth	20 MHz
BS radius	5,000 m
BS transmission power	47 dBm
RS transmission power	44 dBm
Noise power	−102 dBm
BS/RS antenna	Omni-directional
Frame duration	10 ms

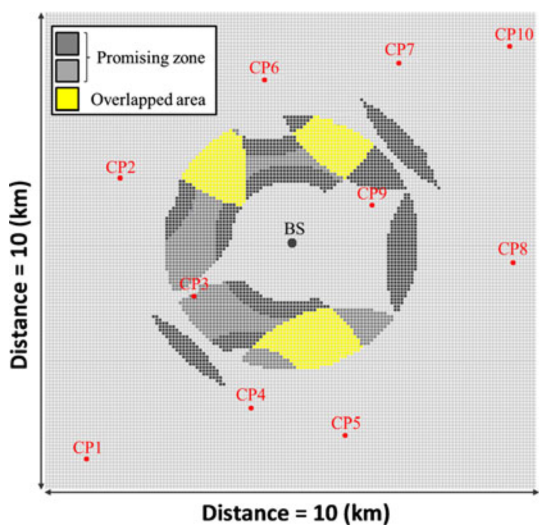

Fig. 20 A screenshot of network environment

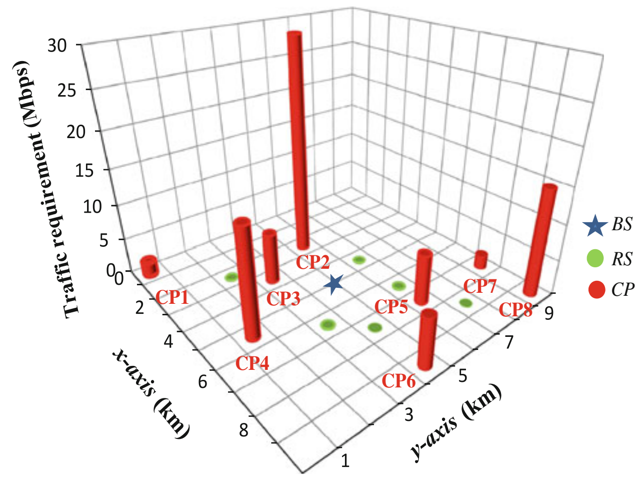

Fig. 21 The results by applying the operations of *PZR* phase of the proposed *CARD* algorithm

considered region. Since the network topology is randomly deployed, we conduct 100 runs for each setting. The service types only consider UGS and rtPS connections. Assume that the whole considered region is consisted of ten unequal-size subareas. Therefore, the locations and requirements of 10 *CP*s can be determined by applying Expression (1). The average traffic requirement of all *CP*s is set by 6 Mbps. As shown in Fig. 20, the regions marked by light gray and dark gray colors denote the promising zones of *CP*s with MCS pairs (16QAM1/2, 16QAM 1/2) and (16QAM 3/4, 16QAM 1/2), respectively. The intersection area of neighboring *CP*s is marked by yellow color.

Figure 21 illustrates the simulation results by applying the *PZR* phase of the proposed *CARD*. The x-axis and y-axis, ranging from 0 km to 10 km, represent the coordinates of service region. The location of *BS* is set at the center of the region and marked by a star symbol. According to the network environment given in Fig. 20, the promising zones of CP_2 and CP_6 can be merged to form a larger promising zone by applying the operations designed in *PZR*. Similarly, the promising zones of CP_4 and CP_5 are merged. Hence, the number of promising zones of all *CP*s is reduced to six. In addition, the traffic requirement of new merged CP_2 is the sum of the traffic requirements of original CP_2 and CP_6. Similarly, the traffic requirement of new merged CP_4 is the sum of the traffic requirements from original CP_4 and CP_5. As shown in Fig. 21, the number of *CP*s has been reduced to eight *CP*s. The z-axis denotes the traffic requirement of each *CP*s. The *RS*s (marked by green spot) are determined to be deployed at the center of each promising zone. As a result, the number of deployed *RS*s can be reduced since the promising zones can be merged into a larger one by applying the proposed *CARD*.

Though the proposed *PZR* phase determines six *RS*s to be deployed in the green spots, however, the number of *RS*s actually deployed in the serving region can be further reduced by applying the proposed *MRA* phase. As shown in Fig. 22, the z-axis denotes the normalized *relay benefit* calculated by applying Expression (16). The proposed *MRA* phase finally determines four *RS*s (marked by green color) to be actually deployed in the serving region, where the *RS*s RS_5 and RS_6 (marked by blue color) are removed for saving the deployment cost. By applying the proposed *CARD*, the RS_1 and RS_2 are determined to be deployed prior to the other two relays because they adopt better MCS for transmitting data and thus serve more *CP*s than the RS_3 and RS_4. Compared with RS_2, RS_1 needs to forward more

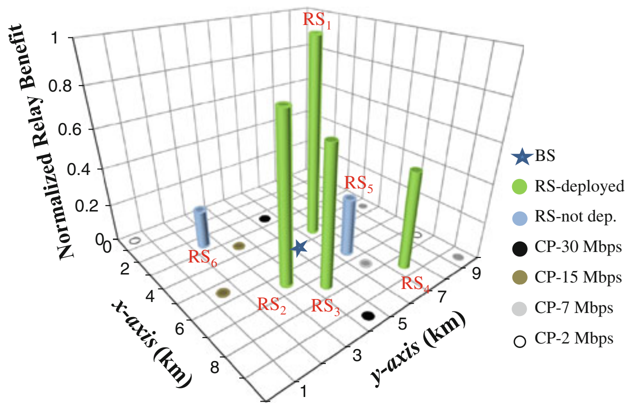

Fig. 22 The final decision by applying the proposed *CARD* algorithm. There are four relays actually deployed in the serving region of the *BS* for supporting the required traffics of 10 *CPs*

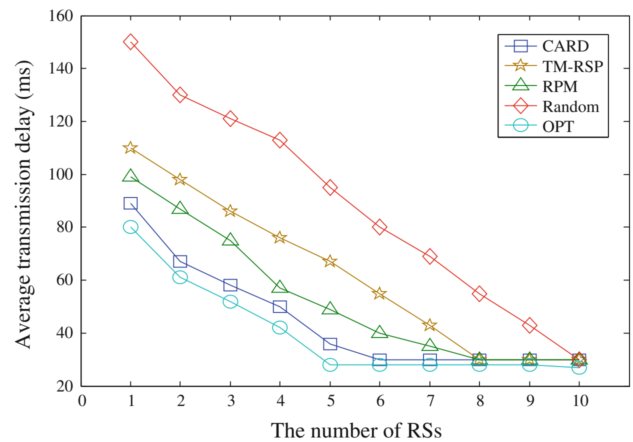

Fig. 24 The comparison of the proposed *CARD* and the other four schemes in terms of average transmission delay by varying the number of deployed *RS*

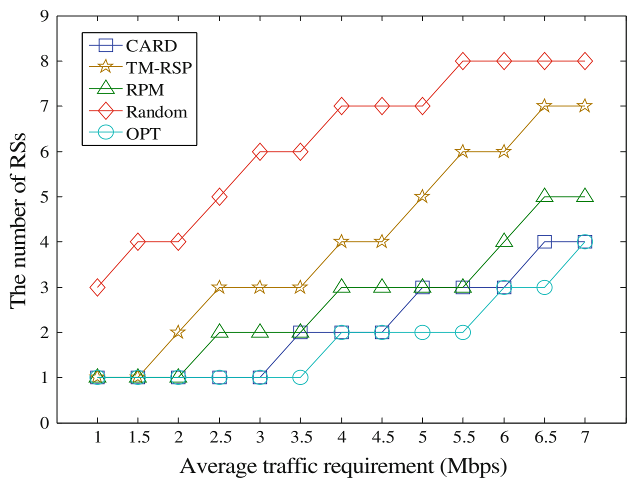

Fig. 23 The relation between the average traffic requirement and the number of *RS*s in the networks

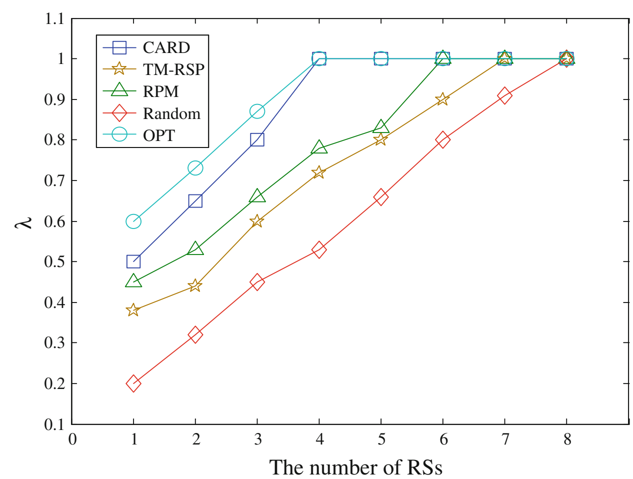

Fig. 25 The comparison of the proposed *CARD* and the other four schemes in terms of QoS Satisfactory Index λ versus the number of *RS*s

data from its serving *CP*s to *BS*. Hence RS_1 has the largest value of relay benefit and can significantly increase the network throughout. In addition, the proposed *CARD* determines that relays RS_5 and RS_6 need not to be deployed because the total traffic requirement of all *CP*s has been satisfied.

Figure 23 compares the proposed *CARD* with *TM-RSP* [14], *RPM* [15], *Random* and *OPT* schemes in terms of the number of *RS*s. In general, the numbers of required *RS*s of the four compared mechanisms are increased with the average traffic requirement. The major reason is that deploying *RS* could improve the transmission rate and hence higher traffic requirement needs to deploy more relays. In general, *CARD*, *TM-RSP* and *RPM* outperform the *Random* scheme. The *Random* scheme randomly determines the locations of *RS*s in the promising zones and thus leads to a situation that two *CP*s might not share the common relay. Hence the *Random* scheme needs a larger number of *RS*s as compared with the other three schemes. When the average traffic requirement is larger than 1.5 Mbps, *CARD* and *RPM* deploy smaller number of *RS*s than *TM-RSP*. This is because that both *CARD* and *RPM* determine the deployment locations by considering all possible locations in the serving region, instead of some predefined candidate locations. When the average traffic requirement is larger than 2 Mbps, the proposed *CARD* approach outperforms the other three mechanisms since the *Minimal Number RS Allocation Phase* always deploys the *RS*s at the best locations for increasing the contribution of each *RS* in rate enhancement. Therefore, the performance of proposed *SADP* is closed to that of *OPT*.

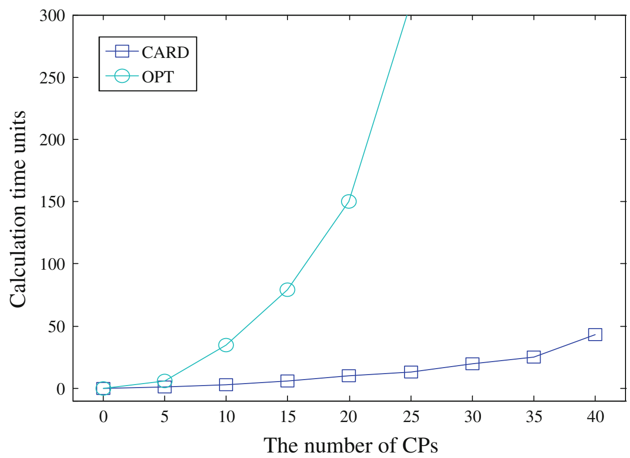

Fig. 26 The comparison of *Promising Zone construction phase* and *OPT* in terms of calculation time

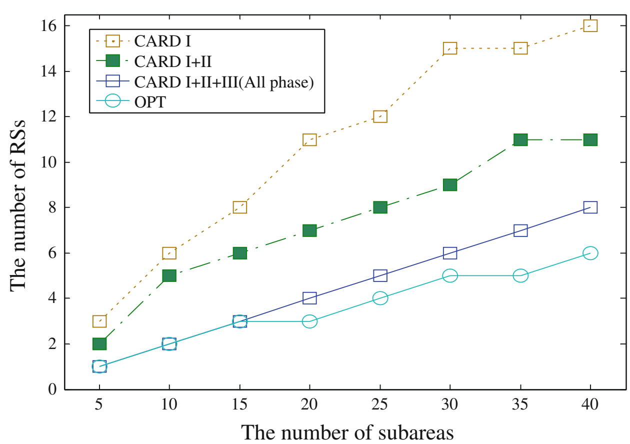

Fig. 27 The investigation of the impact of each phase on the number of relays

Figure 24 further investigates the average transmission delay by applying the proposed *CARD* and the other four schemes. The traffic requirement of each *CP* ranges between 5 and 15 Mbps. At the beginning, the average transmission delay is high. However, the average transmission delay is decreased with the number of *RS*s. This result reveals that deploying *RS*s at the appreciate locations can improve the network throughput and hence reduce the delay. In general, our proposed *CARD* outperforms the other three schemes in terms of the transmission delay. Notice that when the number of *RS* is six, the transmission delay of *CARD* cannot be further improved. This is because that the deployment of six relays has satisfied the traffic requirements. To achieve the same transmission delay with the proposed *CARD*, the *TM-RSP*, *RPM* and *Random* schemes need to deploy more *RS*s. This is because that the other three mechanisms cannot deploy the *RS*s at the best location where more than one *CP*s can share the same relay. Hence, the proposed *CARD* obtains less transmission delay than the other compared mechanisms. It is notable that the transmission delay of the proposed *CARD* approaches to that of the *OPT*. Furthermore, the *Random* scheme results in longer transmission delay than the proposed *CARD*, *TM-RSP* and *RPM* because that some *RS*s are deployed in the improper locations.

Figure 25 further investigates the performance of five compared mechanisms in terms of the satisfactory index of QoS requirements of *CP*s. Let $|C|$ denote the number of *CP*s. Let ω denote the number of *CP*s whose QoS requirements are satisfied by the deployment of relays. Expression (18) defines the QoS Satisfaction Index λ.

$$\lambda = \frac{\omega}{|C|} \tag{18}$$

The larger value of λ means that more traffic requirements of *CP*s are satisfied from the deployed *RS*s. The simulation environment applied in this investigation is similar to Fig. 20. The average traffic requirement of all *CPs* is 7 Mbps and the traffic requirement of each *CP* is varied ranging from 5 to 10 Mbps. In general, the value of λ is increased with the number of *RS*s. When the number of deployed *RSs* is small, most QoS requirements of *CPs* cannot be satisfied. However, when the number of deployed *RS*s grows, the value of λ achieves one which indicates that the traffic requirements of all *CP*s are satisfactory. In general, the proposed *CARD* mechanism outperforms the other three deployment schemes. This is because that the *CARD* determines the locations for deploying *RS*s with better relay benefit. In addition, the compared *TM-RSP*, *RPM* and *Random* schemes need to deploy more *RS*s than the proposed *CARD* to satisfy the QoS requirements of all *CP*s. The major reason is that the proposed *CARD* mechanism considers the relay benefit and the most feasible locations. The proposed *CARD* deploys the relay with the largest value of relay benefit and thus more QoS requirements of *CP*s can be satisfied. Therefore, The QoS Satisfaction of the proposed *CARD* is closer to *OPT* than other three schemes.

Figure 26 measures the calculation time by applying the proposed *CARD* and *OPT* method. We vary the number of *CP*s from 0 to 40. Since the *OPT* method considers each possible location and checks whether or not deploying one *RS* at that location can satisfy the constraint (6). Consequently, it consumes a considerable of time. Recall that the proposed *PZC* phase of *CARD* can collect all feasible MCS pairs and then partition the communication regions of the *BS* and each *CP* into several coronas. Hence, the promising zone can be constructed by the intersection of *BS*'s corona and *CP*'s corona. The MCS pair applied to a certain promising zone indicates the fact that deploying the *RS* at any location of the zone will have the identical benefit. Therefore, the proposed *CARD* does not check all locations of a promising zone. Compared with the *OPT* method, the operations designed in *CARD* significantly reduces the computing time.

The proposed *CARD* approach mainly consists of three phases, including *PZC*, *PZR* and *MRA* phases. Figure 27 measures the impact of each phase on the number of deployed *RS*s. The *CARD* $I + II + III$ (*All_Phase*) denotes the approach that involves the three phases for determining the locations of relays. The *CARD-I* only adopts Phase I to construct the promising zones and then deploys the relay stations at random locations until the requirements of all users are satisfied. The *CARD* $I + II$ additionally involves the operations of Phase II which efficiently reduces the number of promising zones and then deploys *RS*s at random locations. The number of subareas considered in the simulation is ranging from 5 to 40. In general, the number of *RS*s increases with the number of subareas. The *CARD* $I + II + III$ (*All_Phase*) has better performance than the others that involve fewer phases and approaches the performance of *OPT*. The simulation results depict that each phase designed in *CARD* has significant impact and phase III has the most significant impact on the network throughput.

6 Conclusions

The network planning of relay deployment cannot only improve the network throughput but also reduce the cost of deploying *BS* in the WiMAX networks. This paper proposes a relay deployment algorithm for IEEE 802.16j multi-hop relay networks. For a given traffic requirement of each subarea, the proposed *CARD* mechanism determines the best location for relay deployment while the number of required relays is likely minimized. The proposed *CARD* mainly consists of three phases. The *PZC* phase aims to construct a promising zone for each *CP* while the *PZR* phase further merges promising zones to form a larger region, aiming at reducing the computation cost. Finally, the *MRA* phase aims to minimize the number of relays while the QoS requirement of each *CP* is satisfied. Simulation results reveal that the proposed *RS* placement algorithm outperforms existing schemes in terms of the number of *RS*s, transmission delay and QoS Satisfaction Index.

References

1. Oh, S. M., & Kim, J. H. (2011). Application-aware design to enhance system efficiency for VoIP services in BWA networks. *IEEE Transactions on Multimedia, 13*(1), 143–154.
2. AbuAli, N., Hayajneh, M., & Hassanein, H. (2010). Congestion-based pricing resource management in broadband wireless networks. *IEEE Transactions on Wireless Communications, 9*(8), 2600–2610.
3. Tamimi, A. K. A., In, C. S., & Jain, R. (2010). Modeling and resource allocation for mobile video over WiMAX broadband wireless networks. *IEEE Journal on Selected Areas in Communications, 28*(3), 354–365.
4. IEEE 802.16 Working Group. (2009). Part 16: Air interface for fixed and mobile broadband wireless access systems–multihop relay specification, IEEE Standard.
5. Wang, H., Jia, W., & Min, G. (2011). Effective channel exploitation in IEEE 802.16j networks for maritime communications. *IEEE International Conference on Distributed Computing Systems (ICDCS)*.
6. Lu, H. C., & Liao, W. (2011). On cooperative strategies in wireless relay networks. *IEEE International Conference on Computer Communications (INFOCOM)*.
7. Hong, C. Y., & Pang, A. C. (2009). 3-Approximation algorithm for joint routing and link scheduling in wireless relay networks. *IEEE Transactions on Wireless Communications, 8*(2), 856–861.
8. Sundaresan, K., & Rangarajan, S. (2009). Efficient algorithms for leveraging spatial reuse in OFDMA relay networks. *IEEE International Conference on Computer Communications (INFOCOM)*.
9. Kim, Y., & Sichitiu, M. L. (2011). Optimal max–min fair resource allocation in multihop relay-enhanced WiMAX networks. *IEEE Transactions on Vehicular Technology, 60*(8), 3907–3918.
10. Liu, Q., Zhou, S., & Giannakis, G. B. (2005). Queuing with adaptive modulation and coding over wireless links: Cross-layer analysis and design. *IEEE Transactions on Wireless Communications, 4*(3), 1142–1153.
11. Yu, Y., Murphy, S., & Murphy, L. (2008). Planning base station and relay station locations in IEEE 802.16j multi-hop relay networks. *IEEE Consumer Communications and Networking Conference (CCNC)*.
12. Wang, L. C., Su, W. S., Huang, J. H., Chen, A., & Chang, C. J. (2008). Optimal relay location in multi-hop cellular systems. *IEEE Wireless Communications and Networking Conference (WCNC)*.
13. Lu, H. C., Liao, W. (2009). Joint base station and relay station placement for IEEE 802.16j networks. *IEEE Global Communications Conference (GLOBECOM)*.
14. Lu, H. C., Liao, W., & Lin, F. Y. S. (2011). Relay station placement strategy in IEEE 802.16j WiMAX networks. *IEEE Transactions on Communications, 59*(1), 151–158.
15. Chang, C. Y., Chang, C. T., Li, M. H., & Chang, C. H. (2009). A novel relay placement mechanism for capacity enhancement in IEEE 802.16j WiMAX networks. *IEEE International Conference on Communication (ICC)*.

Author Biographies

Chih-Yung Chang received the Ph.D. degree in Computer Science and Information Engineering from National Central University, Taiwan, in 1995. He is currently a Full Professor with the Department of CSIE at Tamkang University, Taiwan. Dr. Chang served as an Associate Guest Editor of many SCI indexed Journals, including *International Journal of Ad Hoc and Ubiquitous Computing* (IJAHUC 2011 & 2012), *International Journal of Distributed Sensor Networks* (IJDSN, 2012), *IET Communications* (2011), *Telecommunication Systems* (TS, 2010), *Journal of Information Science and Engineering* (JISE, 2008) and *Journal of Internet Technology* (JIT, 2004 & 2008). He was an Area Chair of *IEEE AINA*'2005, *TANET*'2000, *TANET*'2010, Vice Chair of *IEEE WisCom*'2005, *EUC*'2005 and *IEEE ITRE*'2005, *IEEE AINA* 2008, Program Co-Chair of *IEEE MNSA*'2005, *UbiLearn*'2006, *WASN*'2007, *ACM SAMnet*'2008, *IEEE AHUC*'2008, *iCube*'2010, *iCube*'2011, Workshop Co-Chair of *MSEAT*'2003, *MSEAT*'2004, *IEEE INA*'2005, *ICS*'2008, *NCS*'2009, *IEEE VCNA*'2009 and Publication Chair of *MSEAT*'2005 and *SCORM*'2006. Dr. Chang is a member of the IEEE and the ACM. His current research interests include Internet of Things, wireless sensor networks, Ad Hoc wireless networks, and WiMAX broadband technologies.

Ming-Hsien Li received the B.S. degree in Computer Science and Information Engineering from Aletheia University, Taiwan, in 2006, and the M.S. degree in Computer Science and Information Engineering from Tamkang University, Taiwan, in 2008. Currently, he is working toward his Ph.D. degree in Department of Computer Science and Information Engineering at Tamkang University. Mr. Li received several scholarship grants in Taiwan and has participated in many wireless sensor network projects. His current research interests include Internet of Things, wireless sensor networks, Ad Hoc wireless networks, and WiMAX broadband technologies.